JOURNAL OF MATERIALS SCIENCE 33 (1998) 5427–5432

Test methodology for the thermal shock characterization of ceramics

V. R. VEDULA, D. J. GREEN, J. R. HELLMANN, A. E. SEGALL*
*Departments of Materials Science and Engineering, and *Engineering Science and Mechanics, The Pennsylvania State University, University Park, PA 16802, USA*

An experimental methodology is proposed to evaluate the thermal shock resistance of ceramics. A technique based on infrared heating has been developed to perform systematic and well controlled thermal shock experiments. This novel technique was used to evaluate the resistance of yttria-stabilized zirconia–alumina foams to thermal loads. Foams of varying cell sizes were subjected to thermal shock and the damage was evaluated using retained strength and non-destructive elastic modulus measurements. The transient thermal gradients and the resulting thermoelastic stresses in the foams were predicted using finite element analysis and the extent of damage was correlated to the maximum thermal strains generated in foams. © *1998 Kluwer Academic Publishers*

1. Introduction

Ceramics are typically subjected to severe thermal loadings during service. Although, a number of techniques have been developed to induce and quantify the extent of damage in ceramics [1, 2], an understanding between the extent of damage and different levels of thermal shock is far from complete. More recently, a thermal shock and fatigue methodology has been developed for ceramic tubes using a combination of acoustic emissions, strength measurements and finite element modelling [3]. The most common technique to evaluate the thermal shock resistance of ceramics is by a down-quench test, where the sample is quenched into water (or some other media) from an elevated temperature. The decrease in a property, such as elastic modulus or strength, is measured as a function of quench temperature difference. This change in the property is then used to quantify the extent of damage in the material. The main drawback of this technique is that it is too simplistic as the material may not be subjected to the temperature gradients and thermal stresses it experiences in actual service. It is therefore difficult to extrapolate the laboratory tests to rank the materials and to predict the damage behaviour under a different set of thermal loads. Hence, an experimental methodology needs to be developed that would enable a better understanding of the relationship between thermoelastic stress and various damage mechanisms that may operate during thermal transients. This paper describes the thermal shock testing of ceramics by a new technique based on infrared heating and a forced-air quench. Thermal shock behaviour of open cell yttria-stabilized zirconia–alumina (YZA) foams has been evaluated using this technique.

Open-cell materials or foams consist of a three-dimensionally interconnected network of beams that are often termed struts [4] (Fig. 1). Ceramic foams have been considered for a variety of uses as a result of their low weight and high fluid permeability. Applications include molten metal filters to remove particulate impurities from aluminum- and iron-based melts. These materials also have potential applications as radiant burners for industrial heating equipment. In these applications, foams are subjected to very high temperatures and large thermal gradients. A knowledge of their thermal shock and fatigue behaviour is, therefore, essential for a reliable performance in such applications.

2. Experimental procedure

2.1. Materials studied

Thermal shock behaviour of commercially available open cell YZA foams (Selee Corporation, Hendersonville, NC) was evaluated in this study. These foams are available with cell sizes ranging from 0.5 to 2.5 mm. In this study, the cell size of the foams was 1.0, 1.7 and 2.5 mm. Foams were characterized for their chemical composition, phase analysis, density and microstructure in the as-received condition. The manufacturer supplied data and subsequent X-ray diffraction results showed that the samples consisted of monoclinic, tetragonal and cubic zirconia (combined total of 63 wt %), and α-alumina (balance). The bulk density was determined using the mass of the sample and specimen dimensions. The elastic modulus of foams was measured by dynamic resonance [5] and the strength was measured in three-point bending. The mechanical properties of three different cell sizes of YZA used in this study and their respective density values are shown in Table I. The thermal expansion of foams was determined using a push-rod dilatometer (Orton Dilatometer, Model 1600D, Westerville, OH), whereas the thermal conductivity values were predicted using basic heat transfer concepts, the details of which can be found

TABLE I Mechanical properties[a] of YZA foams

Cell size (mm)	Density (%)	Elastic modulus (GPa)	Bend strength (MPa)
1.0	0.122 ± 0.009	3.46 ± 0.88	2.05 ± 0.15
1.7	0.116 ± 0.006	2.16 ± 0.33	1.63 ± 0.11
2.5	0.140 ± 0.006	2.49 ± 0.21	1.56 ± 0.13

[a]The values are listed as $\pm$ the standard deviation from 20 measurements.

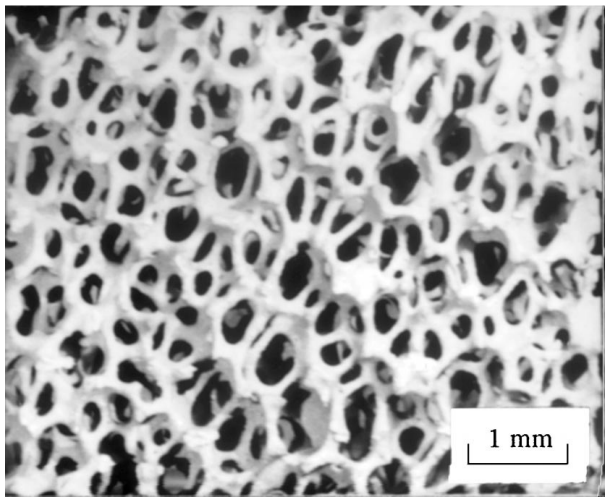

Figure 1 Open-cell ceramic foam.

in [6]. Thermomechanical and thermophysical properties were used to predict thermal gradients and thermoelastic stresses in the foams during thermal shock.

2.2. Thermal shock methodology and damage evaluation

In order to perform systematic and well controlled thermal shock experiments, an apparatus based on infrared heating was developed. A schematic of the equipment is shown in Fig. 2. In this apparatus, the specimens were irradiated from both sides using high density tungsten quartz lamps and the cooling was obtained by forced-air jets. The infrared heaters (Model No. 5208, Research Inc., Minneapolis, MN) had six tubular quartz lamps arranged in a compact array to produce up to 1080 kW m^{-2} of radiant energy on the sample. The large heat flux capability made rapid heating to high temperatures easily attainable. Immediate quartz lamp emitter response provided efficient sample heating within seconds after the power was applied (approximately 90% of output in 2–3 s). Due to the high radiant output from the heaters, it was necessary to cool the units with both air and water. The air cooled the quartz window, lamp endseals and lamp envelopes. The water cooling of the reflector and case body enabled the heat output to stop within a few seconds after the power was removed.

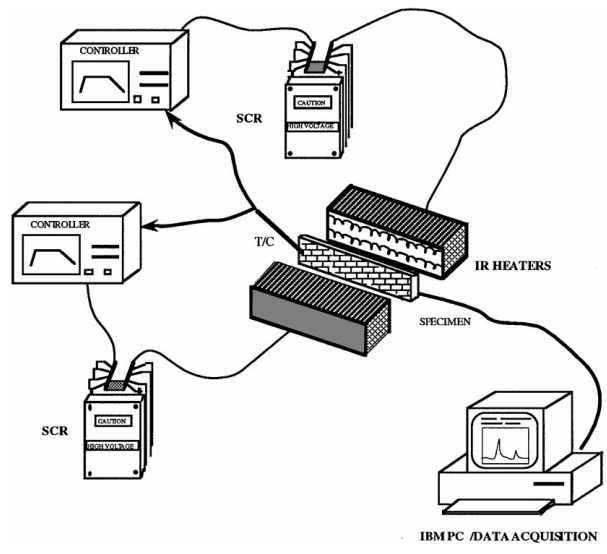

Figure 2 Schematic of thermal shock apparatus.

The temperature profile of the specimen was microprocessor controlled (RedLion Controls, Willow Springs Circle, York, PA), driven by a phase angle silicon controlled rectifier (SCR). The controller received a signal from a thermocouple mounted on a strut surface, displayed the process temperature, and provided an output signal to maintain the desired control point. The temperature controller featured four programmes or thermal profiles, each with up to eight ramp/soak segments. This apparatus allows for extensive control over heating and cooling rates. Moreover, the two heaters can be controlled independently.

In a typical test, a sample was heated from both sides to a selected maximum temperature, held for 2 min and then cooled to room temperature by either natural convection or by forced-air jets directed on the surface of the sample (Fig. 3). The maximum attainable temperature depends on the thermal mass, radiant energy absorption and heat losses from the specimen. High heating rates were achieved when thermal mass and heat losses were low, for example. Fine gauge S and K type thermocouples (wire diameter, 0.005″) were used to monitor the temperature of a strut on the specimen surface and give feedback to the controller. The thermocouples were tied to the struts such that the beads were in immediate contact with the strut surface (Fig. 4). Such a "wrapping" procedure should lead to excellent thermal contact. For this study, the experiments were designed such that during thermal shock, symmetric temperature gradients were generated primarily across the thickness of the foams. During the heating period, the difference between the set temperature and actual temperature depended on the rate of heating. The faster the rate, the larger was the difference, whereas during the hold period, the difference than 5 °C. Temperature measurement at three different locations on the surface of foam showed a maximum differential of less than 20 °C between the centre and edge of the specimen during the hold phase. During the test, the air flow rate for cooling was controlled by the process controller using a combination of solenoid and metering valves. An IBM personal computer with a data acquisition card (Strawberry Tree, Inc., Sunnyvale, CA) was used for recording the temperatures. After thermal shock, the damage in the samples was quantified by the decrease in elastic modulus and strength.

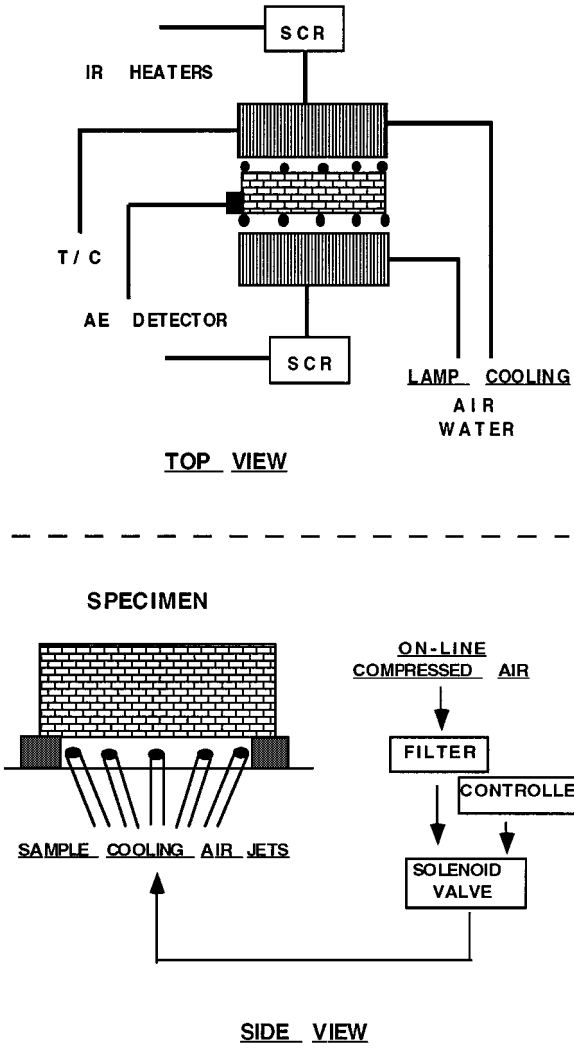

Figure 3 Schematic of cooling arrangement in thermal shock set-up.

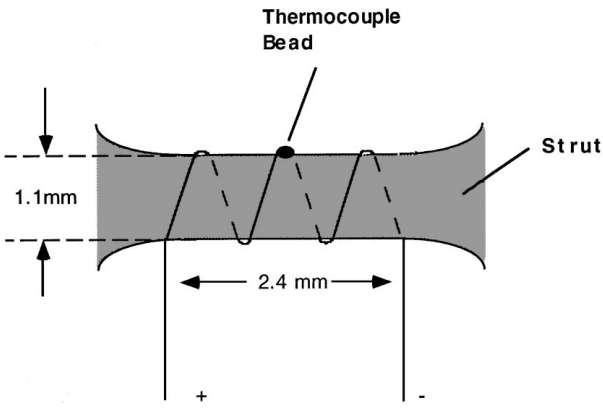

Figure 4 Schematic of a thermocouple tied to a strut.

Non-destructive techniques, such as the measurement of elastic modulus and thermal diffusivity have been previously successful in detecting the thermal shock damage in ceramics [7–9]. In this study, the decrease in the elastic modulus was primarily used to characterize the extent of damage in the materials. The Young's modulus was determined by dynamic resonance [5]. This technique is based on the fact that resonant vibration frequencies of a material depend on the elastic moduli, density and geometry of the material. Therefore, the elastic properties of a material

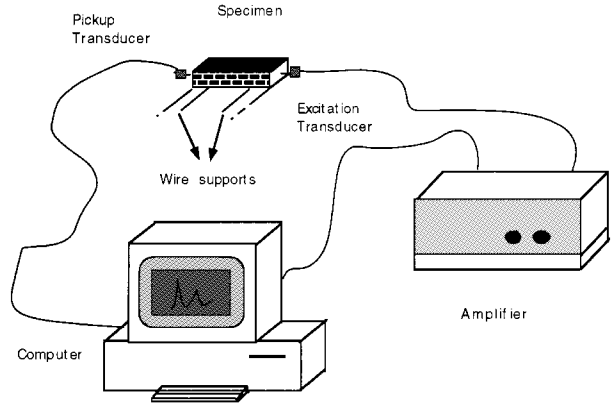

Figure 5 Schematic of elastic modulus measurement set-up.

can be determined if the geometry, density and resonance frequencies are known. This technique involves measurement of the fundamental resonance frequency in the flexural mode. A schematic of the apparatus is shown in Fig. 5. This approach has the advantage over strength testing in that it characterizes the damage throughout the material rather than emphasizing the most severe flaw.

A digitally generated wide band frequency sine wave (24 Hz–25 kHz) was used to excite vibrations at one end of the specimen. The vibration spectra were collected at the other end of the specimen. Excitation and response were created and measured by piezoelectric transducers in contact with the specimen. Resonance peaks were identified by digitally performing the fast fourier transformation (FFT) of the material vibration spectrum using appropriate software (SYSid, Ariel Corp., Highland Park, NJ).

The elastic modulus of the sample is given by

$$E = 0.946\ 45 C m f_f^2 / w \tag{1}$$

where C is a dimensionless shape factor that is a function of specimen dimensions and Poisson's ratio, m is the mass of the sample, w is the width of the sample, and f_f is the fundamental frequency of the flexural vibration mode.

The extent of damage in the foams can be represented by the retained elastic modulus

$$\frac{E}{E_0} = 1 - D_E \tag{2}$$

where E is the elastic modulus after thermal shock, E_0 is the modulus of the as-received sample, and D_E is a damage parameter. D_E can vary from zero in the as-received state to one after thermal shock.

In silicon carbide [6] and alumina [7] foams, it has been shown that the retained elastic modulus and retained strength after thermal shock are linearly correlated. A good correlation between the two parameters suggests that the decrease in the elastic modulus may be used to predict a decrease in the strength of these foams. It is advantageous to use the modulus measurement because it is non-destructive and hence the sample can be used to measure the damage in the "after-shock" condition. In addition, thermal fatigue experiments can

be performed on a single specimen and the cumulative damage determined as a function of the number of thermal cycles.

2.3. Finite element analysis of thermal gradients in foams

During the thermal shock experiments, the samples were heated from both sides and cooled by either natural convection or forced-air jets on the opposite surfaces of the sample. In order to analyse the gradients across the thickness, foams were considered to be a single continuum phase with the same thermomechanical and thermophysical properties as that of the porous material. Thus, the problem simplified to finding a solution for the temperature distributions and thermal stresses in a dense material subjected to convection cooling at both faces.

In the absence of analytical or numerical solutions that could be used to solve the complex transient temperature distribution across the foams, finite element analysis was used for this problem. An advantage of finite element analysis is that the temperature dependent material properties and boundary conditions could be automatically updated within each iteration during the analysis. A commercial package ANSYS (Swanson Analysis Systems, Inc., Houston, PA) was used for this purpose. A three-dimensional isoparametric element with eight nodes (Stiff 70) was used to perform the thermal analysis. Since the samples were cooled from both sides, the problem is symmetric in the thickness direction, and only one-half of the sample was considered for calculations. Thirty-six elements were considered on the face of the sample and five elements in the thickness direction. Due to the nature of cooling, gradients are expected only in the thickness direction, hence a finer mesh was used along the thickness. For the stress calculations, the same nodal geometry was used with an eight node stress element (Stiff 42). The temperature dependent thermal and mechanical properties were entered for automatic extrapolation by the finite element code. The code was validated with an analytical solution for the case of a ramp temperature change at one of the boundaries [6].

3. Results

YZA foams were rapidly heated to 1200 °C at approximately 1000 °C min^{-1}, held for 2 min and cooled to room temperature by forced-air jets on the surface of samples. After thermal shock, the elastic modulus of the samples was measured using dynamic resonance. The variation in the normalized elastic modulus and damage parameter D_E as a function of cell size is shown in Fig. 6. The elastic modulus values are normalized with the elastic modulus of the as-received samples. The values are an average for three samples and error bars represent the standard deviation. As can be seen, the elastic modulus decreases and the extent of damage increases with decreasing cell size.

The microstructure of YZA foams was analysed using a scanning electron microscope (SEM) to determine

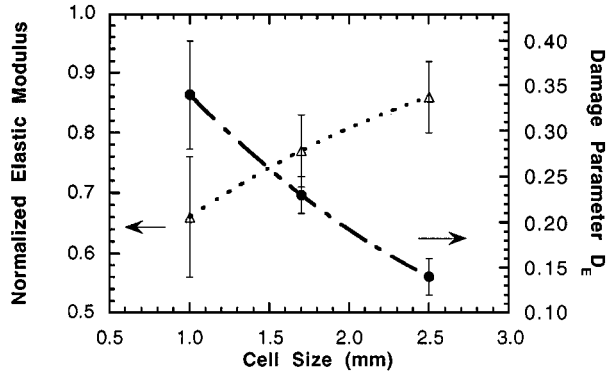

Figure 6 Extent of damage, D_E, versus cell size of YZA foams.

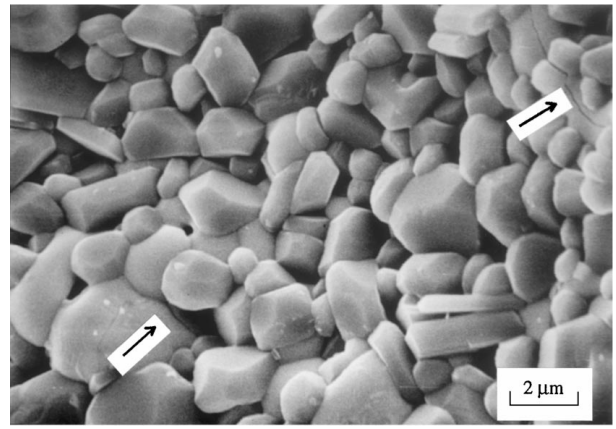

Figure 7 Microstructure of as-received YZA foams showing inter- and intragranular cracks.

the type of damage occurring in the samples. In the as-received state, inter- and intragranular cracks were observed in alumina and zirconia grains in these foams (Fig. 7). Using SEM, it was determined that the crack lengths and the number of cracks increase after the thermal shock. The damage is due to the thermal gradients and thermoelastic stresses generated in foams during thermal shock. Therefore, to gain an insight into the thermal shock behaviour of foams, finite element analysis was used to determine the temperature gradients and magnitude of thermal stresses during the test.

4. Discussion

4.1. Transient thermal and stress analysis

YZA foams were rapidly heated to 1200 °C, held for 2 minutes and cooled to room temperature by forced-air convection. Temperatures were measured at the surface and the interior of the foam to determine the gradients across the thickness during the thermal shock. The measured temperature profile in a 1.0 mm cell size YZA foam is shown in Fig. 8. As can be seen from the figure, there is a finite temperature gradient between the surface and interior of the sample during the heating stage, hold time and the cooling phase of the thermal cycle. These temperature gradients give rise to thermal stresses that induce damage in the samples. During the hold period, the heat loss from the sample edges was responsible for the temperature difference between the surface and centre.

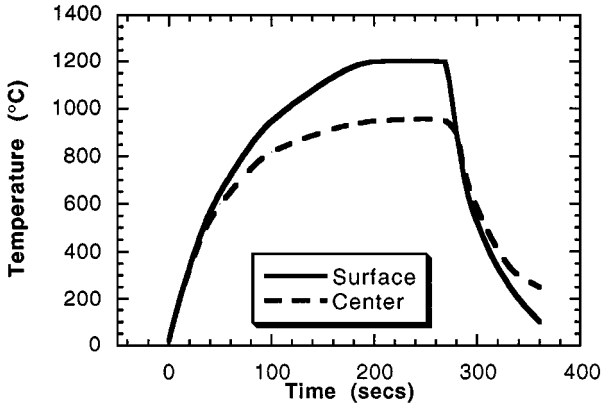

Figure 8 Temperatures at the surface and centre of a 1.0 mm cell size YZA foam during thermal shock.

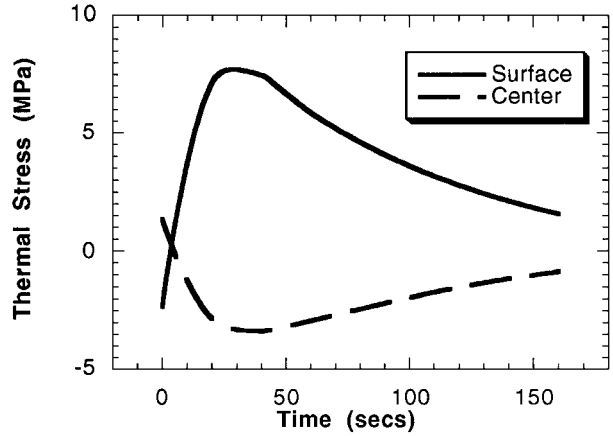

Figure 10 Thermal stresses in 1.0 mm cell size YZA foam subjected to forced convection cooling.

The experiments showed that the heating rate did not have any influence on the extent of damage. Therefore, the damage was induced mainly due to the thermal gradients across the thickness of the samples during cooling. The internal and surface temperature measured experimentally were used to determine the thermal stresses generated in 1.0 mm cell size foams using the finite element code. By fitting the experimental data to calculated temperatures during cooling, the surface heat transfer coefficient required for thermal calculations was determined as 90 $W\,m^{-2}\,K^{-1}$, which is consistent with the values reported in the literature for a solid surface cooled by forced air [10]. Fig. 9 shows the measured and predicted temperatures at the surface and centre of the foam during cooling. The calculations involved piece-wise linear prescribing of the coefficient until the temperatures at the surface and interior matched the measured values. Using the predicted thermal distribution across the sample, the thermal stresses generated at the surface and in the centre were calculated and are shown in Fig. 10. During the heating stage, the surface is under compression whereas the interior is in tension, the latter being at a lower temperature. The stress state remains constant during the hold phase, as shown in the figure at $t = 0$ s. The stresses in the heating stage are not shown in Fig. 10, but were less than 0.4 MPa. During the cooling stage, the stress state reverses and the surface is now subjected to tension. Fig. 10 also shows that the magnitude of stresses generated during cooling at the surface is significantly higher than in the interior. Ultimately, it is these tensile stresses on the surface that are the cause of damage in foams during the thermal shock.

During thermal shock, in addition to thermal gradients across the thickness of foams, gradients are also setup across the individual struts. Finite element analysis was performed to predict the thermal gradients and thermoelastic stresses within struts. The results show that the gradients across the individual struts led to low stresses and are thus not likely the cause of damage, and macroscopic gradients across the thickness of foams are the main source of damage during thermal shock [6].

Fig. 11 shows a comparison of as-received strength and maximum tensile stresses generated at the surface of YZA foams. As can be seen, the strength of foams is fairly independent of cell size, whereas thermal stresses increase rapidly with a decrease in cell size. Thermal conductivity of foams was found to depend very strongly on the cell size of foams, increasing with an increase in cell size, mainly due to an increase in the radiative contribution in large cell size foams [6]. Therefore, the observed increase in tensile stresses with a decrease in cell size is due to the effect of cell size on the thermal conductivity of foams.

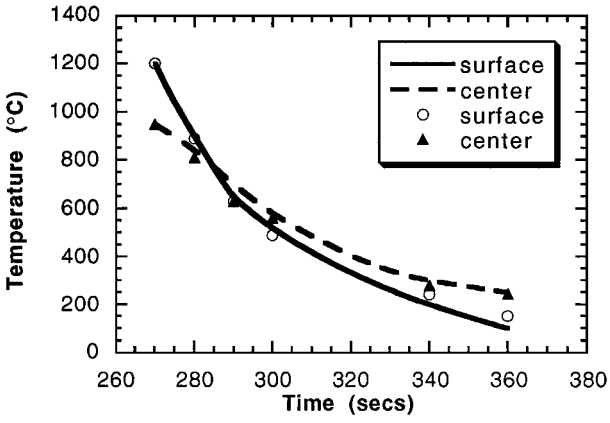

Figure 9 Measured (lines) and finite element analysis predicted (data points) temperatures at the surface and centre of foam during the cooling period.

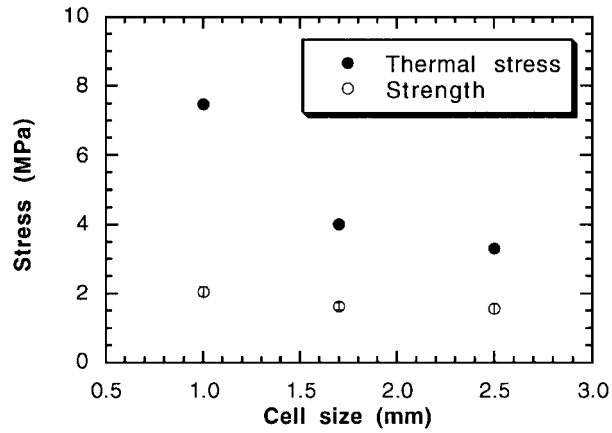

Figure 11 Comparison of as-received strength and maximum thermal stresses as a function of cell size in YZA foams.

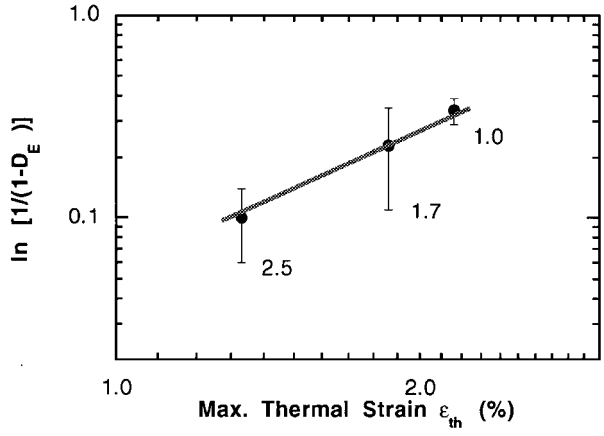

Figure 12 Damage versus maximum thermal strain in YZA foams (the numbers indicate the respective cell sizes in millimetres).

4.2. Thermal stresses versus damage in foams

The extent of damage in foams was found to increase with a decrease in cell size. It was determined that the thermal stresses generated due to temperature gradients across the thickness of foams were the main source of damage in the foams. In order to determine if there was a direct correlation between the magnitude of thermal stresses and the extent of damage, the loss in stiffness, D_E, was expressed in terms of the maximum thermal strain applied to the specimen, ε_{th} (i.e. the ratio of maximum thermal stress to elastic modulus of the undamaged material) using the following empirical equation

$$\ln\left(\frac{1}{1-D_E}\right) = \left(\frac{\varepsilon_{\text{th}}}{\varepsilon_0}\right)^n \tag{3}$$

where n and ε_0 are material parameters that describe the resistance to thermal shock. Since the elastic modulus was found to depend on the cell size, it is advantageous to use the thermal strain instead of thermal stress to compare different cell sizes in a given material. By normalizing thermal stresses with elastic modulus, different materials can also be compared on a single plot.

The damage parameter D_E and the corresponding thermal strains for three different cell size YZA foams are shown in Fig. 12. A very good linear correlation was observed between the extent of damage and thermal strains induced in the foams. By fitting the data to Equation 3, the exponent n was calculated as 1.9.

5. Conclusions

It has been shown that a novel technique based on infrared heating can be used to perform well controlled thermal shock experiments. Experiments on three different cell sizes of YZA foams showed that extent of damage increases with a decrease in cell size. Temperature gradients and transient thermal stresses in foams were predicted using finite element calculations. The results showed that thermal stresses due to bulk thermal gradients were the main cause of damage in foams during thermal shock. Thermal stresses were found to increase with decrease in cell size in YZA foams. A very good correlation between the applied thermal strains and the extent of damage was obtained for the foams. The data suggest that the extent of damage can be represented as a function of applied thermal strains induced in the samples during thermal shock. The experimental methodology described in this paper can also be used for dense ceramics.

Acknowledgements

The authors would like to acknowledge Selee Corporation for providing the foams used in this study. The authors would also like to acknowledge the financial support of Gas Research Institute under grant No. 5093–260–2763 for part of this work.

References

1. K. T. FABER, M. D. HUANG and A. G. EVANS, *J. Amer. Ceram. Soc.* **64** (1981) 296.
2. G. A. SCHNEIDER and G. PETZOW, *ibid.* **74** (1991) 98.
3. A. E. SEGALL, J. R. HELLMANN and R. E. TRESSLER, in Proceedings of the Second International Conference on Ceramics in Energy Applications, London, April 1994 (Pergamon Press, Oxford, 1994) p. 307.
4. L. J. GIBSON and M. F. ASHBY, "Cellular Solids: Structure and Properties" (Pergamon Press, Oxford, 1988).
5. Annual Book of ASTM Standards, Standard C 1198-91, Vol. 15.01 (American Society for Testing and Materials, West Conshohocken, PA, 1996) p. 331.
6. V. R. VEDULA, PhD thesis, Pennsylvania State University, University Park, PA (1997).
7. R. M. ORENSTEIN and D. J. GREEN, *J. Amer. Ceram. Soc.* **75** (1992) 1899.
8. W. J. LEE and E. D. CASE, *Mater. Sci. Eng.* **A119** (1989) 113.
9. H. WANG and R. N. SINGH, *J. Amer. Ceram. Soc.* **79** (1996) 1783.
10. W. D. KINGERY, H. K. BOWEN and D. R. UHLMANN, "Introduction to Ceramics," 2nd ed (J. Wiley, New York, 1976).

Received 4 August 1997
and accepted 30 July 1998